

# Image Cover Sheet

# CA010567

**CLASSIFICATION**

UNCLASSIFIED

**SYSTEM NUMBER**

515355



**TITLE**

DSC/DMA study of poly\(\ether\)urethane thermoplastic elastomers

**System Number:**

**Patron Number:**

**Requester:**

**Notes:**

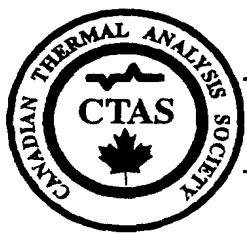
**DSIS Use only:**

**Deliver to:**

*This page is left blank*

*This page is left blank*

---



---

**CANADIAN THERMAL ANALYSIS SOCIETY**  
*AN AFFILIATE OF THE NORTH AMERICAN THERMAL ANALYSIS SOCIETY*

---

**NINTH ANNUAL TECHNICAL MEETING**

**May 17-18, 1999**  
**Mississauga, Ontario Canada**

DSC/DMA STUDY OF POLY(ETHER)URETHANE THERMOPLASTIC ELASTOMERS, John A. Hiltz, Defence Research Establishment Atlantic, Dockyard Laboratory, Building D-17, PO Box 99000, Station Forces, Halifax, NS, B3K 5X5.

### **Abstract**

Poly(ether)urethane thermoplastic elastomers are being considered for use by the Canadian Forces in several applications where their chemical resistance, processibility, and range of temperature and frequency dependent properties lead to reduced costs and improved performance. Poly(ether)urethanes are linear segmented copolymers consisting of urethane rich hard segments and polyol rich soft segments. Incompatibility of the hard and soft segments leads to the formation of hard segment and soft segment domains within the polymer. The degree of phase separation/mixing depends on a number of factors including the structure of the diisocyanate, polyol, and chain extender used to prepare the urethane, the molecular weight of the polyol, the relative proportions of diisocyanate, polyol and chain extender, thermal history and how the elastomer was synthesized. More importantly, the degree of phase mixing affects the properties of the material.

In this paper the results of differential scanning calorimetry (DSC) and dynamic mechanical analysis (DMA) studies of five commercial 4,4'-diphenylmethane diisocyanate/poly(tetramethylene oxide)/1,4-butanediol based poly(ether)urethanes are reported. The results indicate that poly(ether)urethanes with similar compositions have very different levels of phase separation/mixing. This is attributed to differences in the average length of the hard segments in the elastomers that arise from the method used to prepare the polymers.

### Introduction

The tow cable for the Variable Depth Sonar used by the Canadian Navy is faired to improve handling characteristics. Adjacent fairings are tied together with elastomeric

links. The fairing link system is designed to prevent large angle rotation of adjacent fairing. When links fail damage to the fairings occurs during retrieval of the tow cable.

The links used until the early 90s were made from nylon reinforced neoprene rubber. These links had the required mechanical properties but were degraded by the hydrocarbon based water wash resistant grease used to reduce corrosion of the tow cable. To improve chemical resistance and reduce fabrication costs, two thermoplastic elastomers (TPEs), Texin 591-A and Estane 58300, were trialed. Although their chemical resistance was excellent, these poly(ether)urethanes did not have the required mechanical properties. The loads in-service were large enough to cause deformation and failure of the links.

Following the failure of the Texin 591A and Estane 58300 links, DREA was asked to aid in the selection of a thermoplastic elastomer with the required mechanical properties. Five poly(ether)urethanes, were selected for testing. This testing included chemical and thermal analysis characterization of the candidate materials. The dynamic mechanical and differential scanning calorimetry results are presented in this paper.

## Experimental

### Materials

All thermoplastic elastomers were poly(ether)urethanes. Three, Texin 990A, Texin 950D, and Texin 970D, were supplied by Bayer Polymers, Etobicoke, Ontario, and two, Elastollan 1195A and Elastollan 1164D, were supplied by BASF Corporation-Polymers, Wyandotte, Michigan. The last two numbers and the letter in each tradename refer to the Shore durometer hardness and type. For instance, Texin 970D has a Shore type D durometer hardness of 70. Estane 58300, one of the materials tested as a fairing link, was also included in the analysis and was supplied by B. F. Goodrich, Cleveland, Ohio. Estane 58300 had a Shore A hardness of 80.

## Analysis

### Dynamic Mechanical Analysis

Dynamic mechanical analysis (DMA) was carried out on a DuPont Instruments Model 983 Dynamic Mechanical Analyzer. The analyses were done in the fixed frequency mode and the storage modulus ( $E'$ ), loss modulus ( $E''$ ) and  $\tan \delta$  were monitored as the temperature was ramped from  $-80^{\circ}\text{C}$  to  $60^{\circ}\text{C}$  at a rate of  $10^{\circ}\text{C}/\text{min}$ . The glass transition temperature was taken as the maximum in the plot of  $E''$  versus temperature. Test coupons were approximately 42 mm long X 12.5 mm wide X 6.5 mm thick.

### Differential Scanning Calorimetry

Differential scanning calorimetry was carried out on a DuPont Model 2910 Differential Scanning Calorimeter. Samples ( $\sim 10\text{mg}$ ) were heated at a rate of  $10^{\circ}\text{C}/\text{min}$  from  $40^{\circ}\text{C}$  to  $250^{\circ}\text{C}$  and then cooled to  $40^{\circ}\text{C}$  at a rate of  $10^{\circ}\text{C}/\text{min}$ .

### Pyrolysis Gas Chromatography/Mass Spectrometry

Pyrolysis gas chromatography/mass spectrometry (py-GC/MS) analysis of the elastomers was done using a Chemical Data Systems Model 122 pyroprobe coupled to a Fisons Platform II quadrupole GC/MS with a Fisons Model 8000 GC. Approximately  $150\ \mu\text{g}$  of each elastomer was heated at  $20^{\circ}\text{C}/\text{msec}$  to  $700^{\circ}\text{C}$  (20 second dwell time) in a 25 mm quartz tube. The quadrupole MS detector was operated in the full scan mode (25 atomic mass units (amu) to 500 amu).

The pyrolysis products were separated on a 30m long X 0.25 mm inside diameter ARX-5 capillary column with a  $0.25\ \mu\text{m}$  thick stationary phase (5% phenyl-95%dimethylpolysiloxane). The GC was operated in the pressure control mode using Helium (linear flow rate  $0.3\text{m}/\text{sec}$  at  $40^{\circ}\text{C}$ ) as the carrier gas. To reduce deadspace between the pyroprobe and the head of the GC column, the column was threaded up through the pyroprobe interface and positioned adjacent to the end of the pyrolysis tube.

The GC oven was programmed to hold at 40°C for 5 minutes, then ramped at a rate of 10°C/minute to 300°C, and finally held at 300°C for 9 minutes. Total run time was 40 minutes.

### Infrared Spectrometry

Infrared spectra were acquired on a Nicolet Model 510P Fourier Transform infrared spectrometer in the transmittance mode. The spectra were an average of 32 scans and had a resolution of 4 cm<sup>-1</sup>. Thin films of the polymers were laid down on the NaCl plate from a dimethylacetamide solution.

### Results and Discussion

A typical poly(ether)urethane is shown in Figure 1. These are linear segmented copolymers and consist of urethane rich (hard) segments and polyol rich (soft) segments. A schematic representation of a thermoplastic polyurethane elastomer is shown in Figure 2. Agglomerations of hard segments act as the equivalent of cross-links in standard thermoset elastomers. Several factors, including the hard segment content, soft segment length, hard segment length, thermal history, and synthesis method<sup>1,2</sup> affect the degree of separation of the hard and soft phases of these polymers. More importantly, the degree of phase separation affects the properties of the elastomer.

Pyrograms of the six TPEs are shown in Figure 3. Mass spectral identification of degradation products of the TPEs indicated that they were diphenylmethanediisocyanate (MDI)/poly(oxytetramethylene)/1,4-butanediol based poly(ether)urethanes. Differences in the relative percentages of 1,4-butanediol in the Texin 990A, Texin 950D and Texin 970D samples and the Estane 58300, Elastollan 1195A and Elastollan 1164D samples can be seen in the pyrograms. These correlate with the difference in the Shore durometer hardness of the samples and by inference differences in the relative proportions of urethane rich (hard) segments and polyol rich (soft) segments in each pair of elastomers.

Infrared spectra of the TPEs are shown in Figure 4. The peaks at  $1730\text{ cm}^{-1}$  and  $1703\text{ cm}^{-1}$  (non hydrogen bonded and hydrogen bonded carbonyl<sup>3</sup>) and  $1087\text{ cm}^{-1}$  and  $1110\text{ cm}^{-1}$  (C-O stretch soft and hard segment respectively) for the Texin 990A, Texin 950D and Texin 970D indicate hydrogen bonding increases with hardness and that the intensity (concentration) of the C-O polyol stretch decreases with hardness. Similar results are observed for the Estane 58300, Elastollan 1195A and Elastollan 1164D samples. That is, hydrogen bonding increased and the intensity of the C-O polyol stretch decreased with hardness.

#### Dynamic Mechanical Analysis

Plots of  $E''$  versus  $T$  for Texin 990A, Texin 950D, and Texin 970D samples are shown in the top half of Figure 5. Both the temperature of the maximum in the plot of  $E''$  versus  $T$ , which is defined as the  $T_g$ , and the width of the peak in the plot of  $E''$  versus  $T$  increase in going from Texin 990A to Texin 950D to Texin 970D.

Plots of  $E''$  versus  $T$  for Estane 58300, Elastollan 1195A and Elastollan 1164D samples are shown in the bottom half of Figure 5. As was observed for the Texin samples, the  $T_g$  of the soft segments increased and  $E''$  versus  $T$  peak width increased in going from Estane 58300 to Elastollan 1195A to Elastollan 1164D.

The  $T_g$  of the six TPEs are listed in Table 1.

**Table 1**

Glass transition temperature ( $T_g$ ) of the Texin, Elastollan and Estane thermoplastic polyurethane elastomers.

Material	$T_g$ ( $^{\circ}\text{C}$ )
Texin 990A	-25.2
Texin 950D	-7.5
Texin 970D	34.8
Elastollan 1195A	-24.2
Elastollan 1164D	-18.6
Estane 58300	-29.7



The soft segment  $T_g$  increases with hardness for the Texin 990A, Texin 950D and Texin 970D samples. The  $T_g$  of the Estane and Elastollan samples also increase with hardness. It is interesting to compare the increase in  $T_g$  for the Texin and Elastollan samples with similar hardness. The  $T_g$  and hardness of the Texin 990A and Elastollan 1195A are similar. However, the  $T_g$  of the Elastollan 1164D sample is lower than the  $T_g$  of the Texin 950D and Texin 970D samples.

For segmented copolymers the increase in  $T_g$  is consistent with increased phase mixing<sup>3</sup> of the hard and soft segments<sup>1</sup> as the proportion of the hard segments in the elastomers increase. The difference in the Texin and Elastollan samples is strongly suggestive of more phase mixing in the Texin 950D and Texin 970D samples than in the Elastollan 1164D sample.

The broadening of the peak in the  $E''$  versus  $T$  plots may also be indicative of an increase in the heterogeneity<sup>4</sup>, including hard segment length distributions, of the urethanes in going from Texin 990A to Texin 950D to Texin 970D or from Estane 58300 to Elastollan 1195A to Elastollan 1164D.

#### Differential Scanning Calorimetry

Seymour and Cooper<sup>5</sup> observed three endothermic peaks in the DSC traces of MDI/1,4-butanediol based TPEs. They concluded that the three peaks, at approximately 70°C (region I), 160°C (region II), and 180°C (region III), were morphological in origin<sup>6</sup>. The region I endotherm is time dependent and depends on thermal history (annealing temperature). It is attributed to poorly ordered hard segments. The region II endotherm is attributed to more ordered hard segments resulting from microphase separation of the hard and soft segments, and the region III is attributed to the melting of microcrystalline hard segments. Annealing led to changes in the position of the endotherms in regions I and II, that is, the peaks merged to form a single peak on the high temperature side of the

peak in region III. Annealing at temperatures above 200°C led to phase separation of the hard and soft segments and a DSC trace with one endothermic peak. TPEs with low hard segment content do not have an endothermic peak in region III. This may be due to the short hard segment length of the low MDI polymers which affects their ability to crystallize<sup>7</sup>.

The DSC traces for the Texin 990A, Texin 950D, and Texin 970D samples between 40°C and 250°C are shown in Figure 6. The Texin 990A DSC trace had endotherms with minimums at approximately 70°C and 160°C, the latter peak indicating microphase separation of the hard and soft segments of this elastomer. The Texin 950 DSC trace had endotherms with minimums at approximately 70°C, 177°C, and at 200°C. The major endotherm was at 177°C, which is in region III, and indicates the presence of microcrystalline hard segments. The endotherm at 200°C is due the melting of crystalline hard segments resulting from increased phase separation in the elastomer and more long range order in the hard segments. This is consistent with the higher hard segment content of Texin 950D relative to Texin 990A. The DSC trace for Texin 970D has three endotherms at approximately 80°C, 186°C, and 200°C. The major endotherm for Texin 970D is at a higher temperature suggesting more long range order in the microcrystalline hard segments than was observed for Texin 950D.

The DSC traces for the Estane 58300, Elastollan 1195A and Elastollan 1164D samples between 40°C and 250°C are shown in Figure 7. The Estane 58300 DSC trace has three endotherms with minimum at 70°C, 100°C, and 145°C. The lack of an endothermic peak in Region III indicates the lack of microcrystalline hard segments and reflects the small percentage of hard segment in this elastomer. The Elastollan 1195A DSC trace has three endothermic peaks at 70°C, 176°C, and 187°C. The peaks at 70°C and 176°C are similar to those found for Texin 950D. However, the peak at 187°C (shoulder on the larger peak) was not observed for Texin 950D. This arises from domains in the hard phase of Elastollan 1195A with more long range order. The Elastollan 1164D trace has 5

endothermic peaks at 145°C, 176°C, 187°C, 203°C and 220°C. The peaks at 203°C and 220°C may result from domains in the hard phase with more order than is found in the other elastomers.

The differences in the DSC and DMA results for the Elastollan 1164D and Texin 970D TPEs suggest there may be a difference in the hard segment length distributions in the two polymers<sup>2</sup>. This could be due to the way in which the two elastomers were synthesized. Miller et. al. investigated the effect of single and multistep synthesis methods on the properties of MDI/butanediol/poly(oxytetramethylene) thermoplastic elastomers. They concluded, on the basis of IR, DSC and DMA results, that a multistep synthesis resulted in polymers with a higher percentage of hard segments containing a single MDI unit. Because short hard segments are more soluble than long hard segments in the soft phase, the multistep polymers exhibited a higher degree of phase mixing. Conversely, polymers made using a single step synthesis had a lower percentage of hard segments containing a single MDI unit and were therefore less soluble in the soft phase. This resulted in less phase mixing and increased hard domain crystallinity.

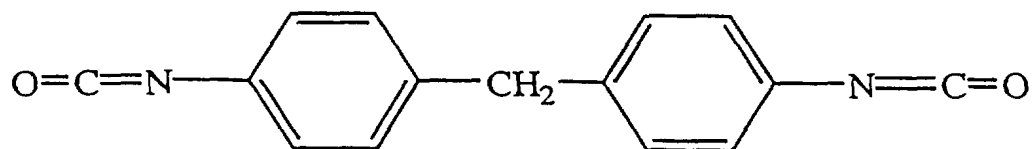
### Conclusions

DMA and DSC analysis show differences in the structure of poly(ether)urethanes that is not evident from chemical analysis techniques such as py-GC/MS and FT IR. In particular, these techniques reveal differences in the degree of phase mixing (separation) of the hard and soft segments of TPEs with similar stoichiometry. Knowledge of these differences is important in applications where dynamic mechanical response and acoustic performance in certain temperature and frequency ranges is critical.

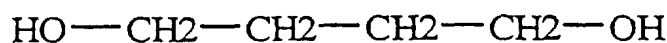
### **References**

1. Y. Li, T. Gao, J. Liu, K. Linliu, C. Richard Desper, and B. Chu, *Macromolecules*, **25**, 7365, 1992.
2. J. A. Miller, S. B. Lin, K. S. Hwang, K. S. Wu, P. E. Gibson, and L. S. Cooper, *Macromolecules*, **18**, 32 (1985).
3. R. W. Seymour, G. M. Estes, and S. L. Cooper, *Macromolecules*, **3**, 579, 1970.

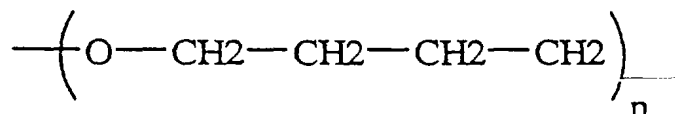
4. T. Murayama, *Dynamic Mechanical Analysis of Polymeric Material*, Material Science Monographs, 1, page 92, Elsevier, New York, (1978).
5. R. W. Seymour and S. L. Cooper, *Journal of Polymer Science*, Polym. Lett. Ed., 9, 689 (1971).
6. R. W. Seymour and S. L. Cooper, *Macromolecules*, 6, 48 (1973).
7. A. K. Sircar, Chapter 5, *Elastomers*, page 1129, in "*Thermal Characterization of Polymeric Materials, Second Edition*", E. A. Turi Editor, Academic Press, Toronto (1997).



MDI



Butanediol



Poly(oxytetramethylene)



Poly(ether)urethane

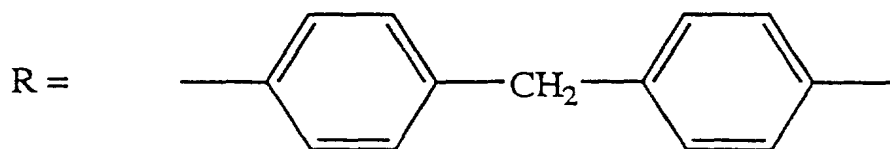


Figure 1 - Starting materials and structure of a MDI/butanediol/poly(oxytetramethylene poly(ether)urethane.

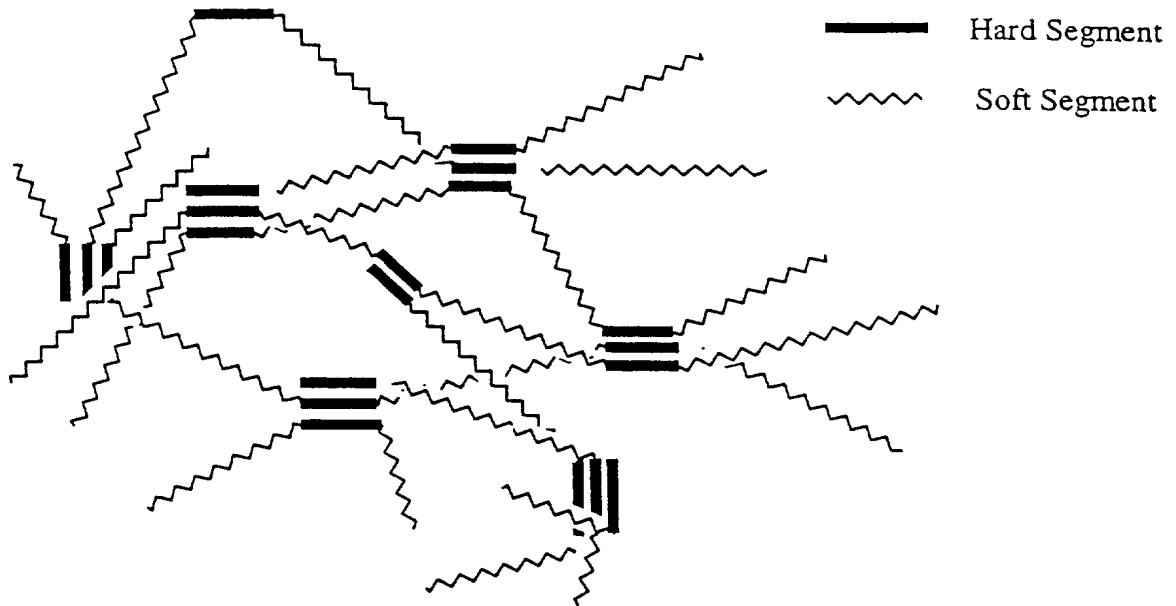


Figure 2 - Schematic representation of a virtually cross-linked thermoplastic poly(ether)urethane elastomer. The hard segments consist of the diisocyanate extended with the diol while the soft segments consist of the macroglycol coupled with the diisocyanate.

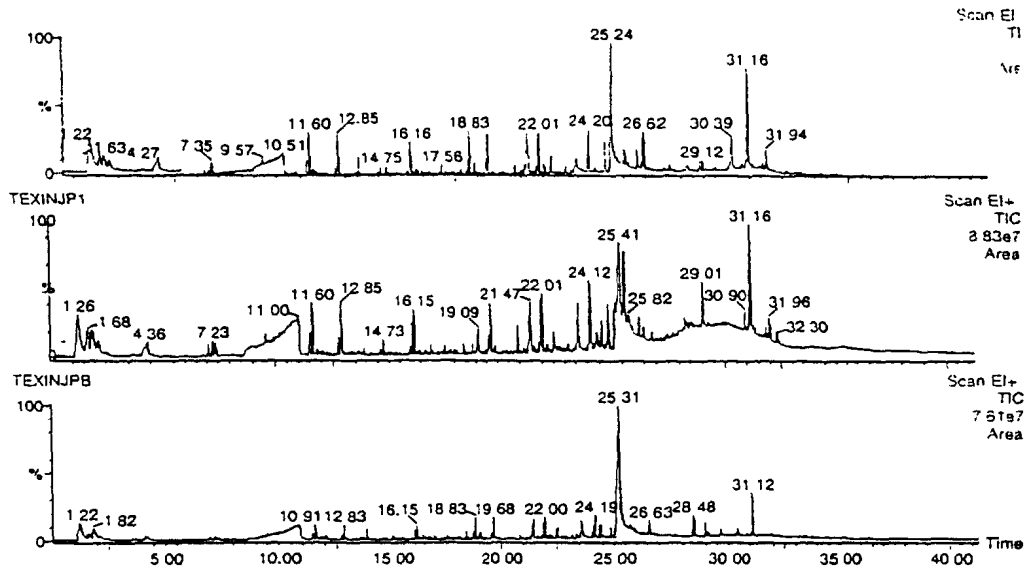


Figure 3a - Chromatograms of the pyrolytic degradation products of top) Texin 990A, middle) Texin 950D, and bottom) Texin 970D following pyrolysis at 700°C.

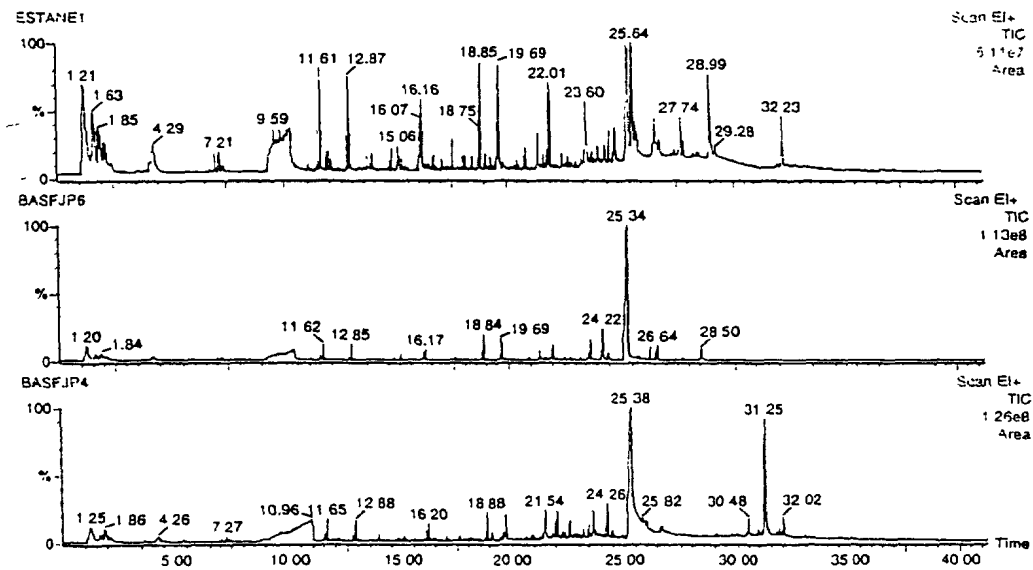
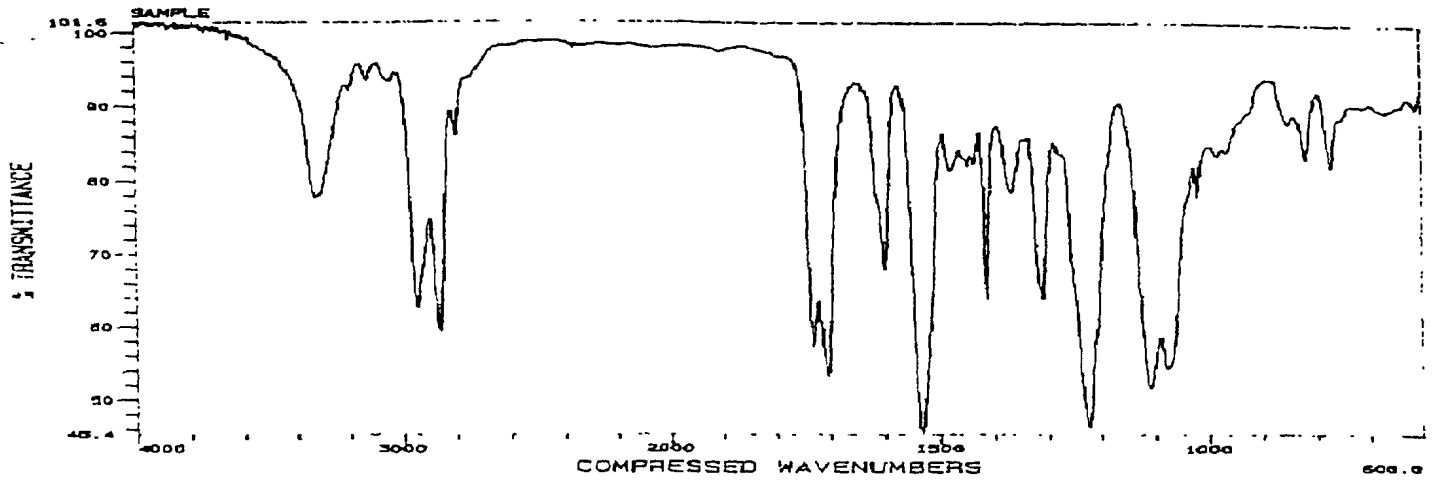
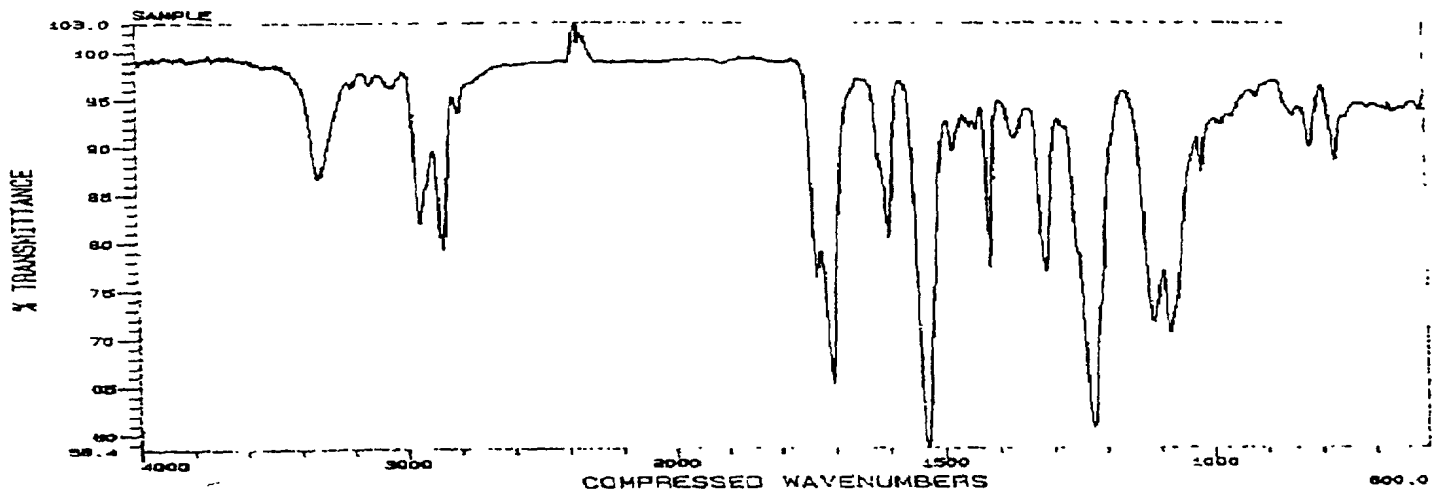


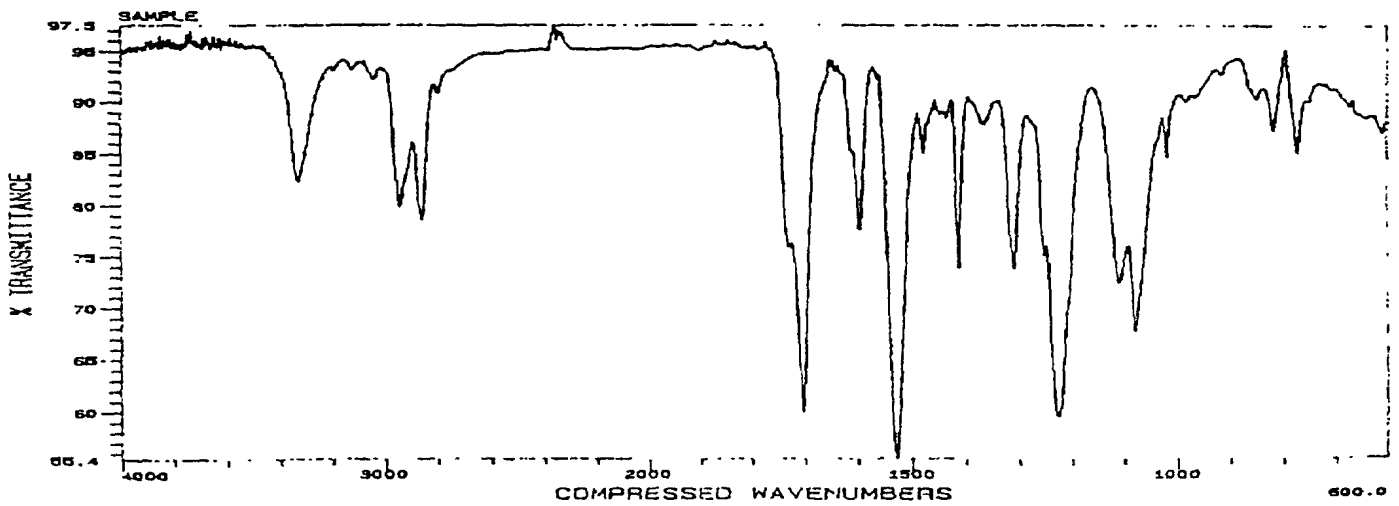
Figure 3b - Chromatograms of the pyrolytic degradation products of top) Estane 58300, middle) Elastollan 1195A and bottom) Elastollan 1164D following pyrolysis at 700°C.



Texin 990A

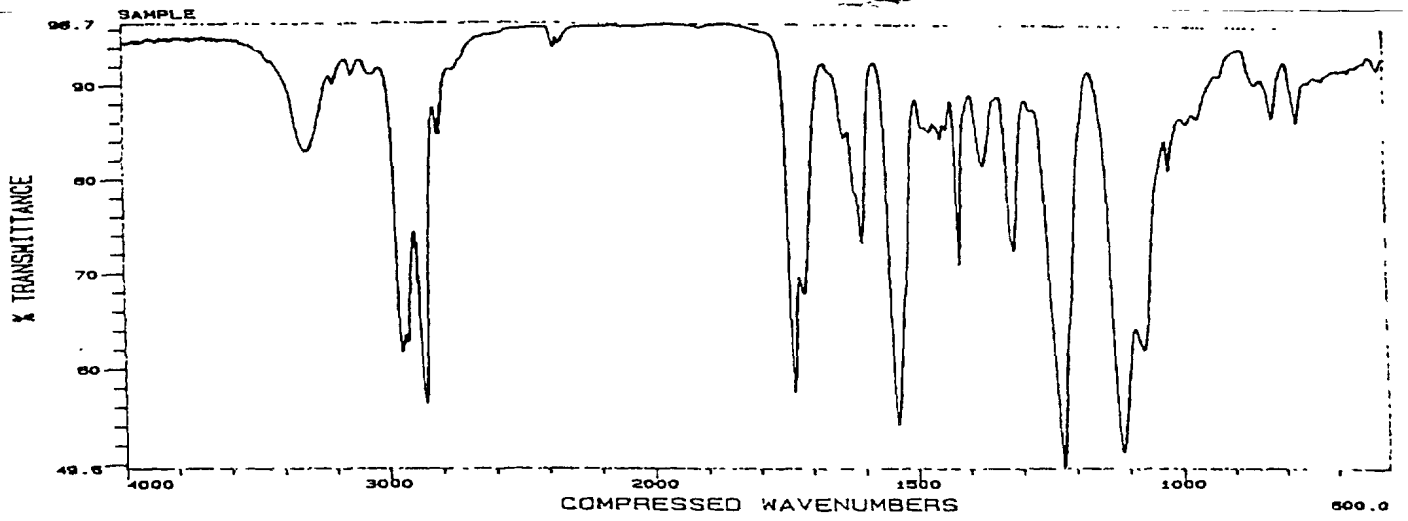


Texin 950D

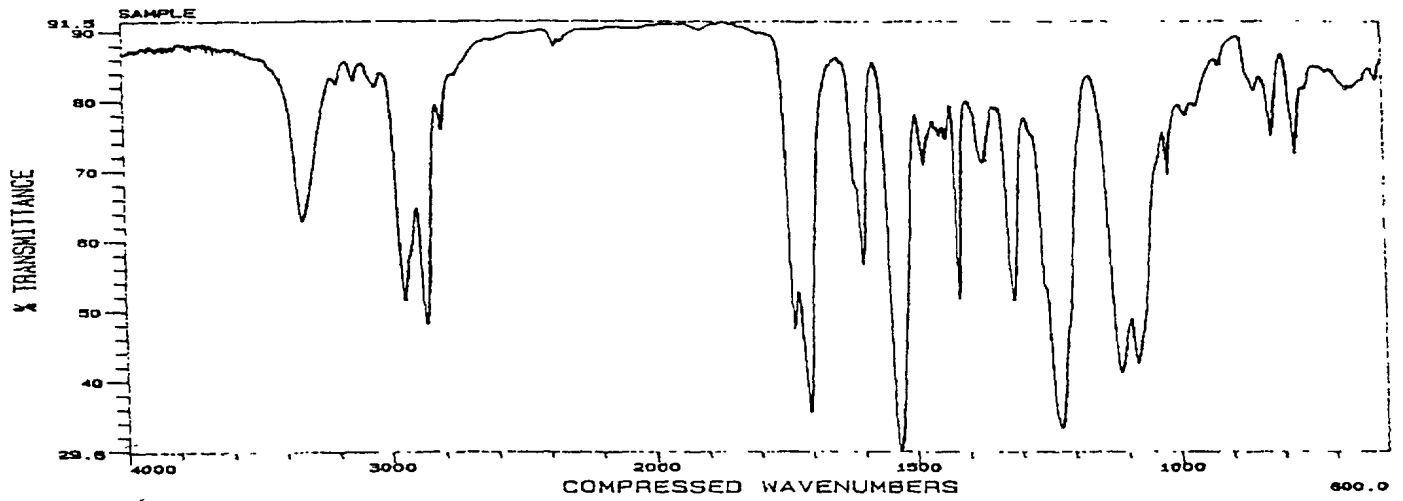


Texin 970D

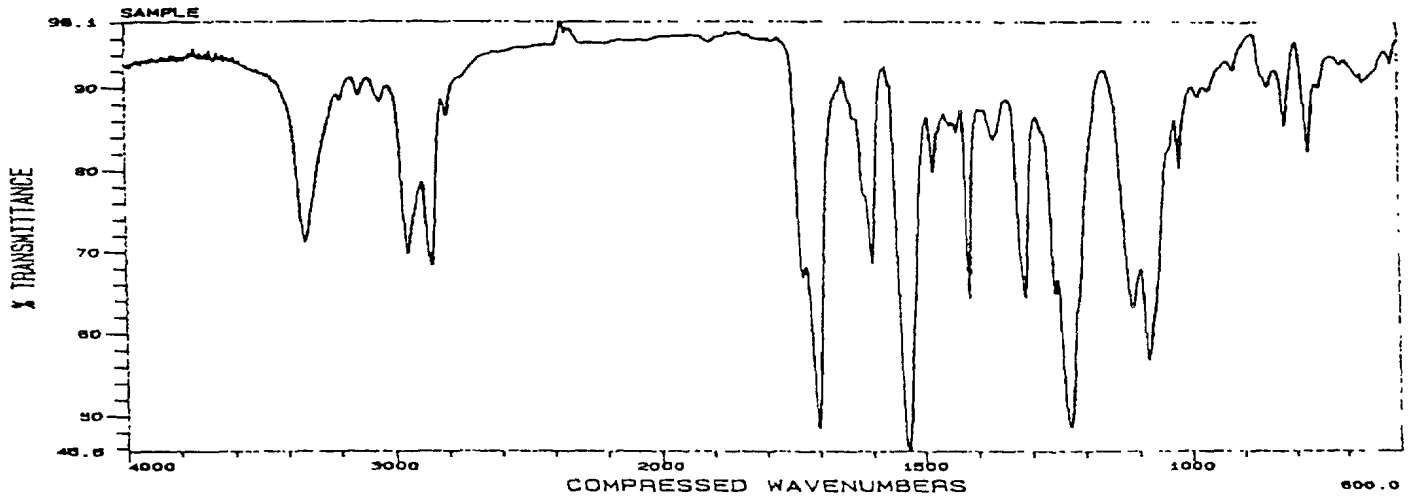
Figure 4a - Infrared spectra of Texin thermoplastic elastomers.



Estane 58300



Elastollan 1195A



Elastollan 1164D

Figure 4b – Infrared Spectra of Estane and Elastollan thermoplastic elastomers.



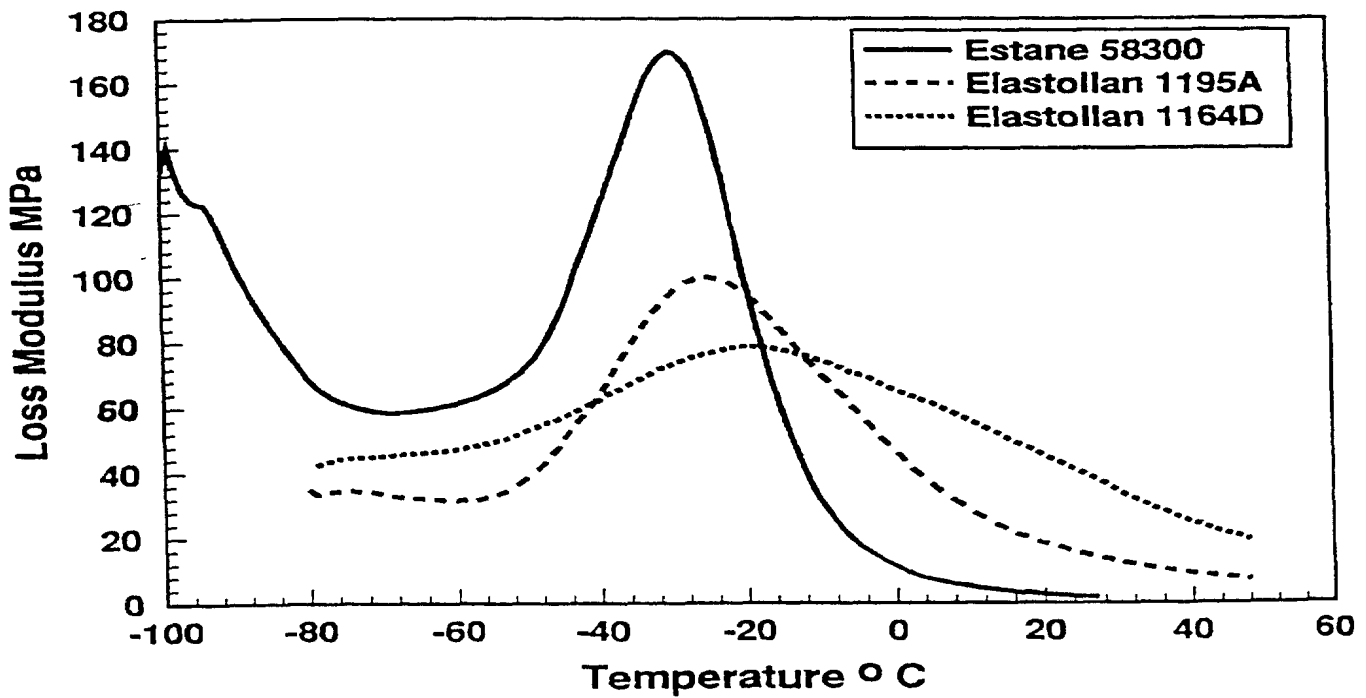
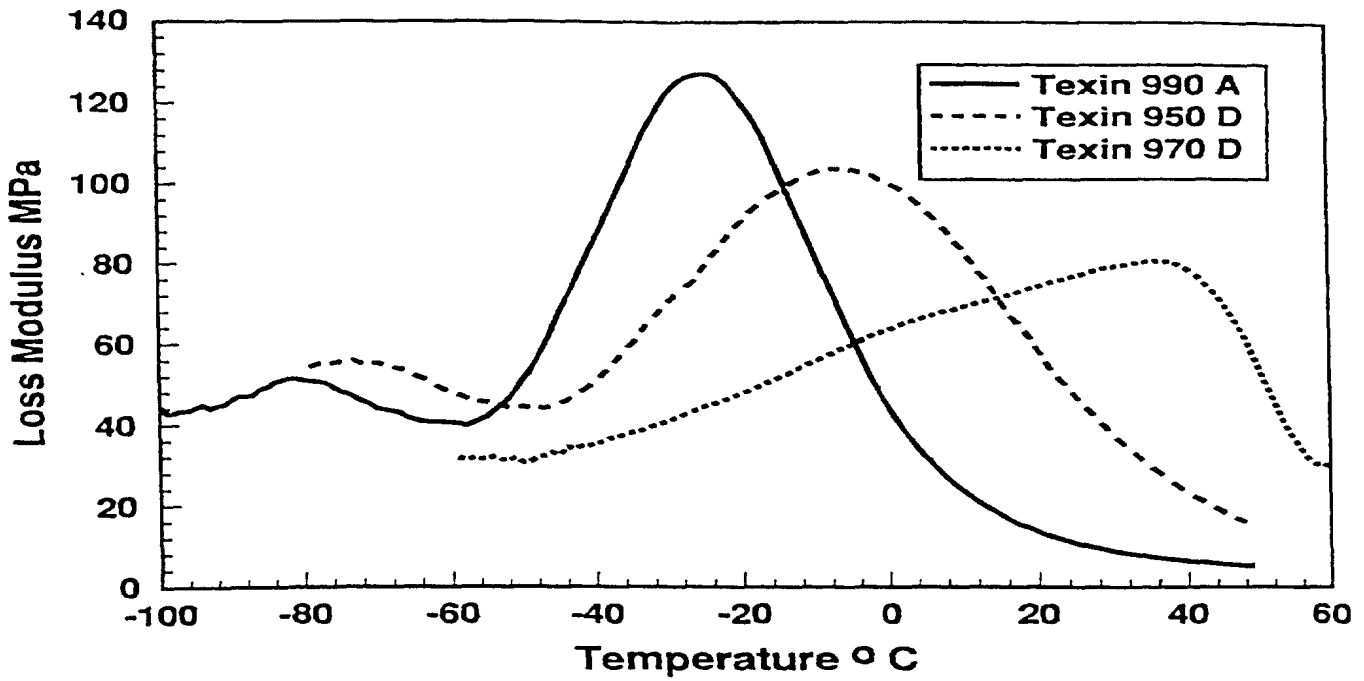


Figure 5 – Plots of  $E''$  versus  $T$  for top) Texin, and bottom) Estane and Elastollan samples.

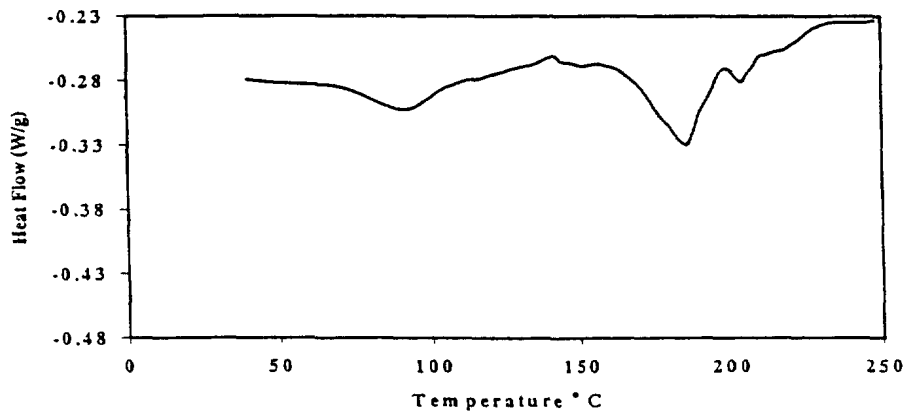
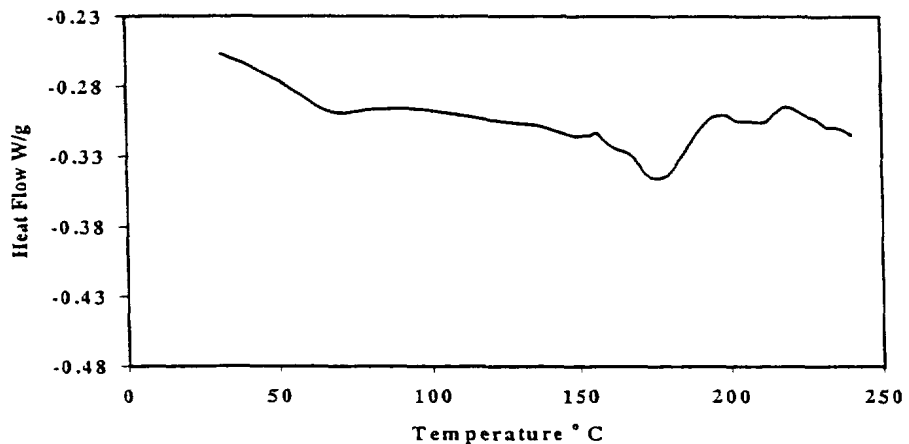
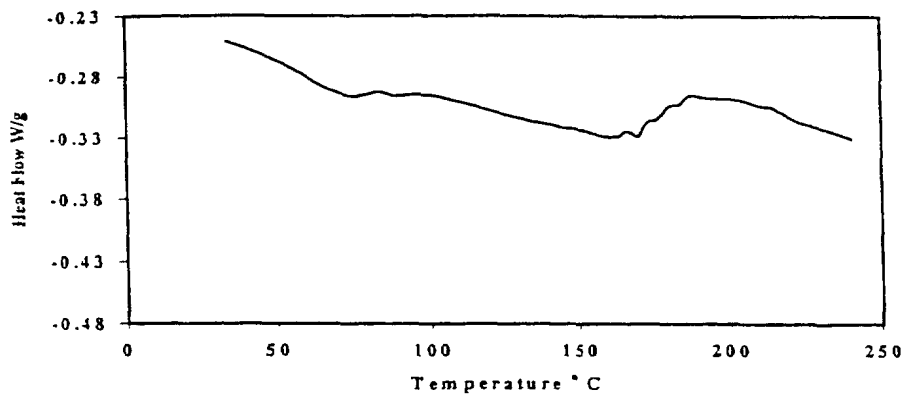


Figure 6 – Thermograms of Texin 990A, Texin 950D and Texin 970D.

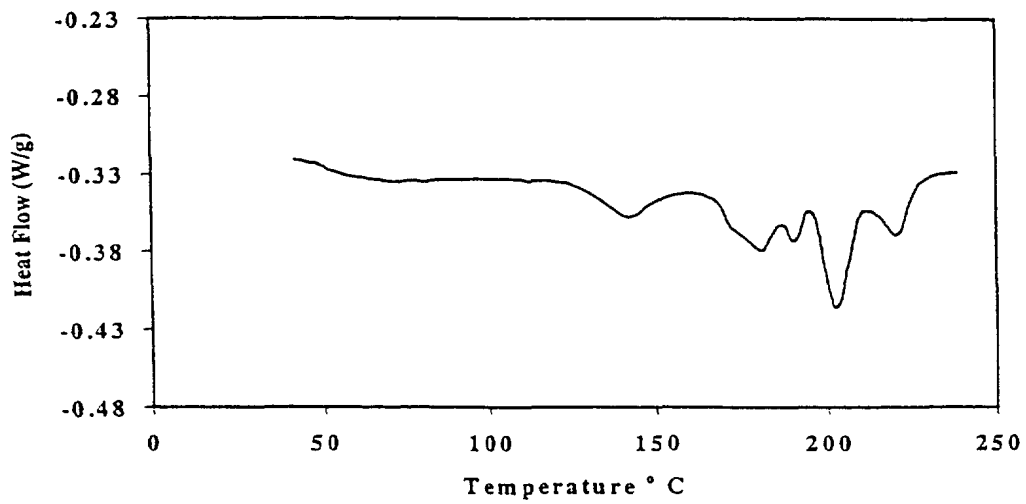
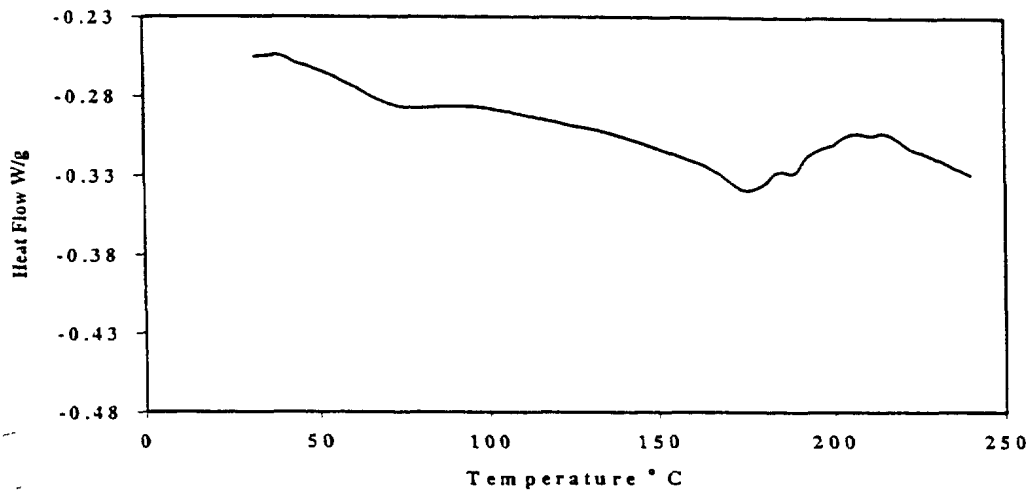
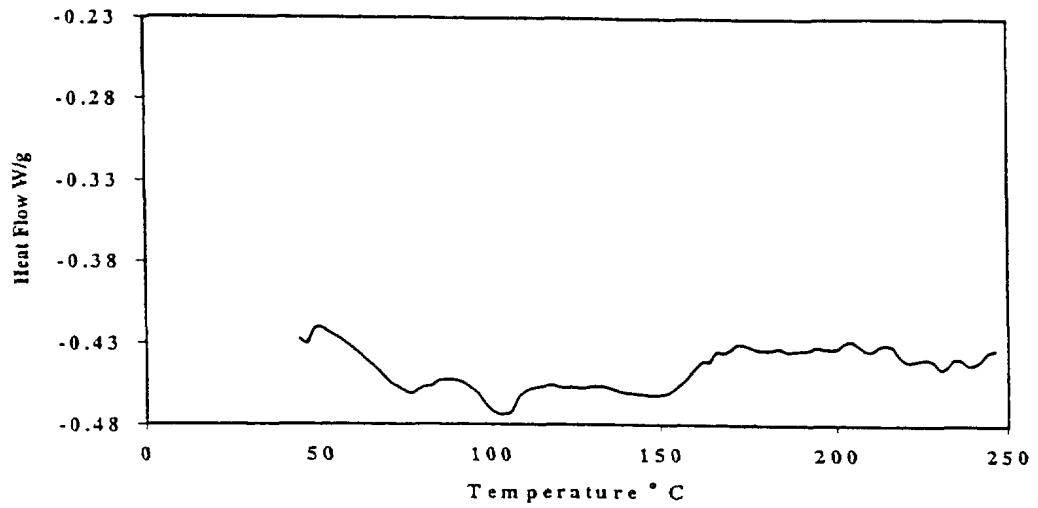


Figure 7 – Thermograms of Estane 58300, Elastollan 1195A, and Elastollan 1164D.

# 515355

CA010567